2-DEOXY-GLUCOSE DOWN REGULATES ENDOTHELIAL AKT AND ERK VIA INTERFERENCE WITH N-LINKED GLYCOSYLATION, INDUCTION OF ENDOPLASMIC RETICULUM STRESS AND GSK-3β ACTIVATION

Krisztina Kovács[1], **Christina Decatur**[2], **Marcela Toro**[1], **Dien G. Pham**[2], **Huaping Liu**[3], **Yuqi Jing**[1], **Timothy G. Murray**[*,2], **Theodore J. Lampidis**[3], and **Jaime R. Merchan**[1,**]

[1]Department of Medicine, Division of Hematology-Oncology, University of Miami Miller School of Medicine and Sylvester Comprehensive Cancer Center

[2]Bascom Palmer Eye Institute, Department of Ophthalmology, University of Miami Miller School of Medicine and Sylvester Comprehensive Cancer Center

[3]Department of Cell Biology, University of Miami Miller School of Medicine and Sylvester Comprehensive Cancer Center

Abstract

Interference with endothelial cell metabolism is a promising, yet unexploited strategy for angiogenesis inhibition. We reported that the glucose analog, 2-deoxy-D-Glucose (2-DG) inhibits angiogenesis at significantly lower concentrations than those required for tumor cytotoxicity. Here, we found that hypersensitivity to 2-DG in endothelial cells is not associated with enhanced drug uptake compared to tumor cells, but with time dependent, endothelial selective inhibition of Akt and Erk phosphorylation. Down regulation of these critical survival pathways is shown to be due to 2-DG's interference with N-linked glycosylation, leading to alterations in VEGFR2 (and downstream signaling) as well as induction of endoplasmic reticulum (ER) stress, GSK-3β activation and apoptosis. In vivo, periocular administration of 2-DG in LH$_{BETA}$T$_{AG}$ mice was associated with significant reduction of newly formed (CD 105 +) tumor capillaries, ER stress (GRP 78 expression), and endothelial apoptosis (TUNEL). These findings uniquely link N-linked glycosylation inhibition, ER stress and Erk/Akt down regulation in endothelial cells, and provide a novel drug development strategy to overcome resistance mechanisms to currently available antiangiogenic agents.

Keywords

angiogenesis; metabolism; n-linked-glycosylation

[**]Address correspondence to: 1475 NW 12th Avenue, Suite 3300. jmerchan2@med.miami.edu.
[*]Current address (TGM): Murray Ocular Oncology and Retina. 6705 Red Road, Suite 412. Miami, FL 33143

INTRODUCTION

The understanding of tumor angiogenesis and subsequent development of vascular targeted agents have revolutionized the treatment of cancer (1). These agents improve clinical outcomes in patients with advanced renal cell carcinoma (RCC), colon, lung, and brain cancers (2-5). However, their long-term benefit is limited, as tumors develop acquired resistance over time (6). Several strategies have been tested to overcome resistance to anti-VEGF agents, including the use of agents targeting VEGF-independent pathways (bFGF, c-MET, IL-8) (7-9), or those responsible for hypoxia-induced tumor responses, such as mTOR (10). Unfortunately, these strategies have not significantly improved long term outcomes in patients with tumors resistant to anti-VEGF agents (10-12). This constitutes a significant challenge in the field of cancer therapeutics, and underscores the urgent need to identify strategies that safely target novel pathways critical for tumor angiogenesis.

It appears that the glucose analog, 2-DG provides such an opportunity. This agent inhibits glycolysis by competitive inhibition with phosphoglucose isomerase and allosteric interference with hexokinase. Due to its similarity to mannose, 2-DG is also known to interfere with N-linked glycosylation by competition with mannose metabolism and by fraudulent incorporation into dolichol-pyrophosphate (lipid)–linked oligosaccharides, which are the precursors of N-linked glycosylation (13, 14). We previously demonstrated that 2-DG significantly inhibits growth, migration, capillary formation and induced apoptosis in growth factor stimulated HUVECs (15), at lower concentrations (0.6 mM) than those needed to induce tumor cell cytotoxicity (16-18). These effects were demonstrated to be due to 2-DG's interference with N-linked glycosylation, rather than glycolysis inhibition. In vivo, 2-DG inhibited neovessel formation in the matrigel plug assay as well as tumor angiogenesis, in the LH$_{BETA}$T$_{AG}$ transgenic retinoblastoma model. In this report, we characterize the molecular mechanisms of endothelial sensitivity to 2-DG. The findings described below provide useful insight into novel mechanisms for angiogenesis inhibition.

MATERIALS AND METHODS

Cell lines and reagents

2-DG, 2-FDG, oxamate, Mannose, Tunicamycin and (2'Z, 3'E)-6-Bromoindirubin-3′-oxime (BIO) were purchased from Sigma-Aldrich (St. Louis MO). Brefeldin A was acquired from Calbiochem-EMD Millipore (Billerica, MA). Matrigel was obtained from BD Biosciences (Bedford, MA) and used at 7mg/ml. Human bFGF and VEGF were purchased from R&D Systems (Minneapolis, MN). Human microvascular endothelial cells from lung (HMVEC-L) was purchased from Lonza (Walkersville, MD) in 2007, used only till passage 5 and was authenticated by vendor. EBM-2 basal medium and the EGM2 and EGM2-MV supplements were purchased from Lonza (Walkersville, MD). Human umbilical vein endothelial cells (HUVECs, purchased 3-4 times yearly depending on usage and used till passage 5), MDA-MB-231(purchased in 2007) and HT-29 (purchased in 2012, 2014) were purchased from the ATCC (Manassas, VA) and were authenticated by vendor. For the endothelial cell experiments described below, "Unstimulated ECs" are defined as cells maintained with endothelial basal medium (EBM) with 1% FBS while "stimulated ECs" are cells that were starved overnight (EBM and 1% FBS), and then treated with either bFGF or VEGF (10

ng/ml) the day of the experiment. Endothelial cell media contains 1 gram of glucose per liter (5.5 mM).

2-DG uptake assay

HUVECs, HMVEC(L)s, HT-29 and MDA-MB-231 cells were seeded in their appropriate media and conditions at 2×10^5 cells per well in 6-well-plates. After incubation, medium was replaced with fresh "hot" medium (high glucose DMEM with 300 μmol/L cold 2-DG and 1 μCi ^{3}H 2-DG -Perkin Elmer, Akron, OH), and the sample was incubated for 5 or 30 minutes at 37°C and 5% CO_2. Medium was then removed, cells were rinsed 3 times (serum-free medium), and lysed with 0.5 mL of 1N NaOH and a 10-second ultra sonication. A 0.25-mL sample was used for protein analysis. Radioactivity from the remaining sample was counted in a Packard CA2000 liquid scintillation spectrometer (Packard tri-carb 2900TR Liquid Scintillation Analyzer). Specific radioactivity was determined by dividing the total radioactivity applied to each sample by the total number of moles of hot 2-DG applied to each sample, as previously reported (17). Results are displayed as nmol/mg of protein (+/− SD), at 5 or 30 minutes.

Matrigel Tube Formation Assay

The matrigel tube formation was performed as previously described (15, 19, 20) . For time course experiments, plates were incubated at 37°C in 5% CO_2; endothelial cell tube formation was assessed at 2, 4, 8 and 18 hrs. with an inverted photomicroscope (Nikon, Melville, NY), and quantification of total tube length was performed as previously described. Experiments were done at least in duplicate and repeated at least twice.

Western Blot analysis

Unstimulated or stimulated endothelial cells, and serum (10%) stimulated tumor cells were treated with 2-DG or other agents, incubated for different time periods and lysed. Protein concentration was determined from lysates by the BCA assay (Thermo Scientific, Rockford IL). 10-20 μg proteins were prepared with 4X Laemmeli sample buffer and separated in 10% or 4-20% Mini-Protean TGX gel (BioRad, Richmond, CA), transferred to 0.45 μm pore sized PVDF membranes (Bio-Rad) and probed (1:1000 dilution) for Akt pSer[473], S6 pSer[240/244], Erk pThr[202]/Tyr[204], GSK-3β pSer[9], PERK pThr[980], cleaved-Caspase-3, cleaved-PARP, total-VEGFR2, VEGFR2 pTyr[1175], and PLC-γ1 pTyr[783] (Cell signaling, Danvers, MA), GSK-3β pTyr[216] (Calbiochem), and GAPDH (1:20,000 dilution) for loading control (Rockland, Gilbertsville, PA). Following probing, membranes were processed as previously described (15, 18). Band intensities of replicate Western blot figures were quantified with ImageJ software, normalized to the corresponding GAPDH bands, and results presented as percentage of control (untreated cells) +/− SEM.

Immunocytochemistry for total VEGFR2 in HUVECs

HUVECs were plated in starving medium in chamber slides (VWR, Radnor, PA) at 80 000 cells per chamber. The following day cells were treated as indicated and incubated for 24 hrs. After incubation, sections were washed with PBS and fixed with 4% paraformaldehyde at room temperature for 1 hr. Cells were then washed 3 times with PBS and blocked with

10% normal serum (goat) in 1% BSA+0.1% TritonX-100 in PBS for 1 hr. at room temperature. Sections were then probed with anti-totalVEGFR2 primary antibody (1:25; Abgent, San Diego, CA) and incubated overnight at 4° C. After 2 washes, Alexa fluor 488 goat anti-rabbit IgG secondary antibody (Invitrogen) was applied (1:500, for 1 hr. at room temperature). This was followed by 3 PBS washes; slides were mounted with anti-fade mounting medium (Molecular Probes, Eugene OR) and analyzed by fluorescent microscopy. Representative pictures were taken with a Zeiss LSM700 confocal microscope at 63X.

N-glycan digestion

HUVECs were seeded on 10-cm dish (4×10^4) and treated with or without 0.6 mM of 2-DG in endothelial cell growth medium, incubated for 24 hrs. and lysed. Protein concentration was determined from lysates by the BCA assay (Thermo Scientific, Rockford IL). Equal amounts of proteins (30 μg) were digested at 37°C in 300-ml reactions with sialidase (Neuraminidase; specificity for a2-3, a2-6, and a2-8 N-acetyl-neuraminic acid residues), endo H (removes only high mannose and some hybrid types of *N*-linked carbohydrates), and PNGase F (removes almost all types of *N*-linked (Asn-linked) glycans: high mannose, hybrid, bi-, tri- and tetra-antennary. New England BioLabs, Ipswich, MA) according to the manufacturer's instructions. After 5 min digestion with sialidase, or 40 minutes with endo H or PNGase F, digested and undigested samples were boiled with 4X Laemmeli sample buffer and analyzed with Western blot for determination of VEGFR2.

In vivo studies

The LH$_{BETA}$T$_{AG}$ transgenic mouse model (21-23) was used to evaluate *in vivo* effects of periocular administration of 2-DG on tumor angiogenesis. Thirteen-week-old mice (n=7 in first experiment and n=8 in second experiment) were treated with either 2-DG (75 mg/kg or 1.5 mg in a 20 gram mouse) or balanced salt solution (vehicle control; Alcon Laboratories, Inc., Fort Worth, TX). Each dose was administered in a total volume of 20 μl via subconjunctival injection in the right eye, twice a week for 2 or 3 weeks (separate experiments). Twenty four hours after final treatment, mice were euthanized and eyes were enucleated for tumor studies.

Immunofluorescence staining for microvessel density

Measurement of tumor vasculature in retinoblastoma samples were performed as previously reported (15, 21), with minor modifications. Briefly, eyes were frozen in O.C.T. immediately following enucleation and serially sectioned (8 μm). Slides were fixed with methanol for 10 minutes (−20°C) before immunohistochemical analyses. Total vessels were detected with biotin-labeled lectin (*Bandeira simplicifolia*, a pan endothelial binding agent; 1:1000, Sigma, St. Louis, MO) and Cy3-conjugated streptavidin (1:500, Sigma). Neovessels were detected with α-endoglin (1:1000, Santa Cruz Biotechnology) and Alexa Fluor 488-conjugated α-IgG2 (1:500, Invitrogen). Omission of the primary antibody (secondary only) was used as a negative control for nonspecific binding. Cell nuclei were stained for 5 minutes with 4′, 6′ diamidino-2-phenylindole (DAPI, 1:5000; Invitrogen). All tumor areas were digitally imaged at 200X magnification with appropriate fluorescent filters on an Olympus BX51 microscope. Fluorescent signal intensities were analyzed separately, and

then merged using Photoshop CS (Adobe, San Jose, CA). Differences in intraocular tumor vasculature between control and treated animals were measured by thorough quantification (in arbitrary units) of lectin or endoglin fluorescence signals within the total tumor area (vessel/tumor ratio) from all micrographs. Tumor vascular densities were displayed as mean percentages of total tumor areas +/− standard error of the mean (SEM).

In vivo assessment of tumor unfolded protein response (UPR) and apoptosis

Tumor samples were processed as above, and 8 μm frozen tumor sections were washed with PBS and fixed with 4% paraformaldehyde at room temperature (RT) for 1 hr. For determination of tumor UPR, sections were fixed as above and slides were washed 3 times and blocked with 10% normal serum (goat) in 1% BSA+0.1% TritonX-100 in PBS for 1 hr. at room temperature. Sections then were co-stained with anti-CD-105 conjugated w/Alexa Fluor 488 (endoglin for angiogenic endothelial cells; dilution 1:50) and anti GRP78 (BiP) antibody (dilution 1:100; Cell Signaling, Danvers, MA) for URP and incubated overnight in the cold room. This was followed by washes and then incubation with the secondary antibody Alexa Fluor 647 (Invitrogen; 1:500 dilution). This was followed by 3 PBS washes and slides were treated with anti-fade mounting medium (Molecular Probes) and analyzed for apoptotic ECs by fluorescent microscopy. Representative pictures were taken with a Zeiss LSM700 confocal microscope at 40X.

To detect and visualize apoptosis, slides were washed twice with PBS (after fixation), permeabilized with 0.2% TritonX-100 for 20 minutes at RT and after 2 additional washes with PBS, sections were probed with label solution (for negative controls) or TUNEL reaction mix, following manufacturer's instructions (in situ cell death detection kit; Roche Applied Science, Indianapolis, IN). Sections then were probed with anti-CD-31 antibody (eBioscience, San Diego, CA 1:50 dilution) and incubated overnight at 4°C. After 2 washes, Alexa Fluor (Red) 555 goat anti-rat IgG(H+L) (Invitrogen) secondary antibody was applied at a 1:500 dilution for 1 hr. at RT. Then slides were washed, mounted and analyzed with confocal microscope as described above.

Laser capture microdissection of tumor tissues

Tumor tissue was isolated from sections obtained from the above experiments. Eight μm sections were placed onto Director Laser Microdissection slides (Expression Pathology, Rockville, MD) and stained with hematoxylin. Areas containing tumor cell nuclei were microdissected, using a Leica AS LMD laser microdissection system. Approximately 50,000 tumor cells were dissected from each section and collected into Eppendorf caps containing 50 μl of Lysis Buffer® with β-mercaptoethanol. GRP 78 expression was determined by immunoblot of LCM protein samples. Protein isolation and immunoblot from LCM samples was performed as described (24).

Statistical Analysis

Data are presented as means +/− SEM. Differences in means among three or more groups were analyzed by analysis of variance (ANOVA). Pairwise comparisons were performed using the Tukey–Kramer method. Means between two groups were compared by Student's t test analysis. Differences were considered statistically significant at $P< 0.05$.

RESULTS

Comparative analysis of 2-DG transport in endothelial and tumor cells

Human endothelial cells (HUVEC, HMVEC) are significantly more sensitive to the cytotoxic effects of 2-DG compared to tumor cells (15). To test the hypothesis that differences in sensitivity to low doses of 2-DG between endothelial and cancer cells are due to differential drug transport, cellular uptake of radioactive 2-DG was measured. Drug transport was not increased in endothelial compared to cancer cells, at 5 or 30 minutes (Table 1). HT-29 cells had significantly higher drug uptake compared to HUVEC (p= 0.0086) and HMVEC (p= 0.0005) at 5 minutes and compared to HMVEC at 30 minutes (p= 0.0002). VEGF or bFGF stimulation modestly (but not significantly) increased 2-DG transport in HUVECs at 1 hour, but not a 24 hours, compared to controls (Table S-1). Growth factor stimulation did not increase 2-DG uptake in HMVECs.

Differential effects of 2-DG on endothelial vs. tumor cell Akt, mTOR and Erk phosphorilation

Endothelial proliferation, capillary formation, migration and survival (all affected by 2-DG (15) are regulated in part by the PI3K/Akt and MAPK pathways (25-27); therefore, we investigated the effects of low dose 2-DG on these pathways in ECs and tumor cells. While no significant effects were observed in HUVECs when treated with 2-DG at 1 hour, at 24 hrs. Akt_{473} (fig. 1.a, d), S6 (fig 1.b, e), and Erk phosphorylation (fig. 1. c, f) were significantly downregulated, and the effects were reversed by co-treatment with mannose. The effects of 2-DG on AKT phosphorylation were more marked in HUVECS treated with bFGF (Fig. 1.d) than with VEGF (fig. 1. a), while pS6 (fig. 1. b, e) and pERK (fig. 1. c, f) down regulation were equally potent in HUVECS stimulated with either growth factor. In contrast, down regulation of these pathways was not observed in MDA-MB231 (fig 2. a, b, c) or HT-29 (fig. 2. d, e, f) cancer cell lines when similarly treated. Erk and S6 were found to be significantly down regulated by 2-DG at 8 hours in HUVECs exposed to either VEGF or bFGF, whereas Akt was mildly increased (Figure 3. a, b, c).

Effects of other glycolytic inhibitors on endothelial Akt and Erk pathways

The finding that 2-DG's inhibition of Akt and Erk is reversible by mannose strongly suggests that these effects depend on 2-DG's interference with endothelial N-linked glycosylation, and not glycolysis. To further support this interpretation, the effects of equimolar concentrations (0.6 mM) of fluoro-deoxygluose (FDG, a more potent glycolytic inhibitor and weaker N-glycosylation inhibitor than 2-DG), and oxamate (a glycolytic inhibitor with no detectable ER stress-inducing activity) on the above pathways were investigated. Neither FDG nor oxamate had effects on Akt or Erk phosphorylation (Figure 3. d, e) whereas FDG, but not oxamate, decreased S6 phosphorylation, albeit to a lower degree compared to 2-DG.

Correlation between the dynamics of Erk down regulation by 2-DG and inhibition of endothelial tube formation

Endothelial capillary formation, disrupted by 2-DG, is a dynamic process that is regulated in part by Erk (25, 27). To determine if the timing of endothelial Erk inhibition correlated with the effects of 2-DG on tube formation, 2-DG treated HUVECs were plated on matrigel and tube formation was observed at 2, 4, 8, and 18 hours. Clear inhibition of endothelial tube formation was observed at 8 hours of treatment, compared to controls, and the effects were more marked at 18 hours. (Figure 4).

Effects of 2-DG on endothelial VEGFR2

The vascular endothelial growth factor (VEGF) promotes angiogenesis by binding to its endothelial receptors, mainly VEGFR2, with subsequent activation of downstream signaling (28, 29). As VEGFR2 undergoes posttranslational N-linked glycosylation (28), we investigated the influence of 2-DG on this receptor.

In HUVECs simultaneously treated with 2-DG, we observed changes in the migration pattern of total VEGFR2 compared to untreated cells. While control cells showed a normal, mature VEGFR2 (migrating at 210-230 kDa), in 2-DG treated cells, VEGFR2 migrated at a lower molecular size (approximately 150 kDA, figure 5. a), consistent with the production of unglycosylated, immature VEGFR2 (28). The observed effects were mannose reversible.

To further investigate whether the shift of VEGFR2 migration induced by 2-DG was due to VEGFR2 hypoglycosylation, we performed selective digestion of HUVEC lysates treated with 2-DG or controls, using N-glycan digesting enzymes (sialidase, endo-H) as well as PNGase F (see methods), and western blot for VEGFR2 was performed. We observed a clear difference in the VEGFR2 digestion patters between control and 2-DG treated cells (fig. 5. b). Control (untreated) samples were sensitive to sialidase (mild decrease in receptor migration, due to removal of terminal sialic acid residues). While the upper VEGR2 band was sensitive to this enzyme as well as PNGase F, the lower band was cleaved by both endoH and PNGase F. On the other hand, VEGFR2 from HUVECs treated with 2-DG were resistant to sialidase treatment and had a similar digestion pattern after both endo H and PNGase F digestion (we observed the presence of intermediate bands in control, but not 2-DG treated cells after digestion with endo H and PNGase F. The significance of those bands is not clear, but may represent partially digested VEGFR2 in the control cells).

To further confirm that changes in VEGFR2 migration pattern were due to interference with N-linked glycosylation, we examined the effects of tunicamycin, an inhibitor of N-linked glycosylation, and Brefeldin A (BFA), an agent that induces ER stress without inhibiting N-linked glycosylation (30). While the glycosylation inhibitors 2-DG and tunicamycin had similar effects on VEGFR2 migration, BFA did not (Figure 5. c). Immunofluorescent determination of VEGFR demonstrated that receptor expression is not inhibited after 2-DG treatment either at 1 of 24-hours after treatment. (Figure 5. d). Even though HUVECs exposed to 2-DG (or the N-linked glycosylation inhibitor tunicamycin) for 24 hours displayed significant changes in cell size and shape (due to apoptosis induced by the drug), receptor expression was observed. The above findings indicate that 2-DG, while not

significantly affecting expression, it interferes with VEGFR2 N-linked glycosylation, leading to an immature, lower molecular weight isoform.

To further investigate the functional consequences of 2-DG-induced changes on VEGFR2, the above treatment conditions were modified: HUVECs were pretreated with 2-DG for 24 hours, before stimulation by VEGF, and immunoblots of pVEGFR2, and downstream signaling mediators were performed 1 hour after stimulation. Under these conditions, 2-DG decreased the levels of total VEGFR2, as expected. Even though phosphorylation of the smaller molecular size VEGFR band was observed, activation of its downstream adaptor PLC-γ1 pTyr[783] was decreased and Akt and Erk were downregulated as compared to control cells (Figure 5. e, f). These effects were attenuated by co-treatment with mannose further indicating that they were due to 2-DG interfering with N-linked glycosylation.

Role of GSK-3β on 2-DG's mediated endothelial apoptosis and pathway inhibition

We have previously shown that 2-DG induces endothelial N-linked glycosylation, leading to induction of ER stress and apoptosis (15). Since glycogen synthase kinase-3 beta (GSK-3β) plays a critical role in ER stress mediated apoptosis (31-33), and reports suggest its involvement in Akt and Erk regulation (34, 35) in tumor cells, we investigated the role of GSK-3β on 2-DG mediated endothelial apoptosis. At 24 hours, 2-DG induced ER stress in HUVECs, as demonstrated by increased levels of phosphorylated PERK and its downstream eIF2α (FIG. 6). Moreover, 2-DG induced GSK-3β activation, as shown by decreased levels of the inhibitory GSK-3β pSer[9] (35, 36) (fig. 6) and were associated with apoptosis, as shown by increased levels of cleaved caspase-3 and cleaved PARP in treated endothelial cells. These effects occurred in HUVECS exposed to either VEGF (fig. 6. a, b) or bFGF (fig. 6. c, d) and were reversed by mannose.

Next, HUVECs were treated with 2-DG in the presence or absence of the GSK-3 β inhibitor Bromoindirubin-3′-oxime (BIO). As shown in figure 7, under these conditions, 2-DG-induced apoptosis was blocked. In addition, BIO partially reversed 2-DG induced Erk downregulation, but did not reverse Akt inhibition. These effects occurred regardless of bFGF (fig 7. a, b) or VEGF (fig. a, c) exposure to HUVECs.

2-DG inhibits tumor neovessels, induces ER stress and apoptosis in vivo

We previously showed that 2-DG inhibits angiogenesis in vivo, in the matrigel plug assay and in the LH$_{BETA}$T$_{AG}$ mouse model of retinoblastoma (15). To further characterize the in vivo antiangiogenic effects of 2-DG, LH$_{BETA}$T$_{AG}$ mice were treated with periocular injections of 2-DG twice a week for 2 weeks as described in methods. In addition to its effects on total (lectin +) tumor vasculature, 2-DG treated mice had a significant reduction of newly formed (endoglin +) microvessels (p= 0.0032), compared to controls (Figure 8. a, b). Repeat experiments, where mice were treated for a period of 3 weeks, showed predominant effects on endoglin positive neovessels, compared to total vessels (figure S-1).

Moreover, tumors of 2-DG treated (but not control) animals demonstrated increased tumor UPR response, as detected by positive GRP78 immunofluorescence (figure 8. C and figure S-2) and immunoblot determination of tumor tissue extracted by laser capture microdissection (figure S-3). GRP 78 positive areas in the 2-DG treated tumors showed co-

staining with CD-105 (endoglin, arrows in figure 8. c). To assess for in vivo apoptosis, the TUNEL assay was performed, along with CD 31 co-staining. Tumors from animals treated with 2-DG showed increased TUNEL positive areas, compared to control tumors (figure 8. d). Additionally, co-localization of TUNEL positive and CD-31 positive areas was frequently found in treated tumors, compared to control tumors (arrows in figure 8.d).

DISCUSSION

When switching from quiescence to angiogenesis, endothelial cells have the ability to adapt their metabolism, allowing them to sustain cell growth and capillary formation in hypoxic microenvironments, in a manner similar to tumor cells (30, 37, 38). This adaptation provides an opportunity to exploit tumor as well as endothelial metabolism for therapeutic gain. 2-DG, which is currently undergoing preclinical and early clinical development for cancer treatment (39-41) inhibits angiogenesis at concentrations significantly lower than those required for tumor cell cytotoxicity(15). In this report, we found that EC hypersensitivity cannot be merely explained on differential uptake since tumor cells were found to accumulate as much or more radiolabeled 2-DG. Rather, we found that EC sensitivity to this agent was associated with endothelial selective down-regulation of Akt and Erk (Figures 1, 2.). These effects were reversible by mannose, and did not occur with oxamate or 2-FDG, indicating that Erk and Akt downregulation is a result of 2-DG's interference with N-linked glycosylation and not glycolysis. Importantly, they were independent of the type of growth factor used to stimulate ECs (i.e. FGF or VEGF) and not observed in the tumor cells tested.

The kinetics of Erk and Akt down regulation were found to be different and correlated with specific biological effects of 2-DG on ECs. Erk (but not Akt) down regulation was observed as early as 8 hours after 2-DG treatment (Figure 2. a), an effect that coincided with inhibition of tube formation, also detected as this time point. Conversely, Akt inhibition was not seen until 24 hours of treatment, which is the time we previously reported that ECs undergo apoptosis when treated with 2-DG (15). These results suggest that 2-DG-induced down regulation of Erk as opposed to Akt may play a more critical role in interfering with tube formation and perhaps with subsequent cell death. Our findings are in agreement with prior reports showing that silencing Erk with SiRNA blocks tube formation, induces cell death in vitro and suppresses angiogenesis in vivo (25, 42, 43). A previous report has shown that high concentrations (25 mM) of 2-DG were found to increase Akt and ERK activation in multiple cancer cell lines (44). These marked differences in endothelial vs. tumor cell regulation of Erk and Akt by 2-DG may therefore explain the increased endothelial sensitivity to this sugar analog.

Our data indicate that 2-DG's interference with endothelial N-linked glycosylation leads to VEGF receptor hypoglycosylation as well as to induction of ER stress, either of which can result in down regulation of Erk and Akt. It is important to emphasize that 2-DG did not reduce VEGFR2 expression, but rather induced receptor hypoglycosylation, as demonstrated by changes in VEGFR2 migration, as well as differential VEGFR2 digestion pattern after treatment with sialidase, endo H and PNGase F. These effects lead to decreased downstream signaling, as shown by lower levels of phosphorylated PLC-γ1, Akt and Erk. The findings that mannose reversed 2-DG's effects on VEGFR2 migration and downstream signaling,

and that tunicamycin also induced similar changes in receptor migration patterns, confirm that the changes were indeed due to interference with N-linked glycosylation. Our observations are in agreement with those of Nacev et al., who found that the antifungal agent itraconazole interfere with VEGFR2 glycosylation, altered receptor trafficking and decrease in cell surface expression and downstream signaling (45). As many endothelial and cell surface receptors involved in anti-VEGF resistance mechanisms, such as EGFR, bFGF, cMET (45-48) are heavily glycosylated, our results suggest that agents that disrupt N-linked glycosylation, such as 2-DG may prove useful in overcoming resistance to current clinically available anti-VEGF agents.

A key observation in this report was the finding that induction of ER stress by low concentrations of 2-DG leads to endothelial apoptosis via activation of GSK3-β. The role of GSK3-β in 2-DG induced apoptosis was confirmed by the results with an inhibitor of this kinase, BIO, which reversed 2-DG-induced endothelial caspase 3 and PARP cleavage (Figure 4. b). This, and the observation that BIO partially reverses 2-DG-induced Erk downregulation, suggest that GSK3-β is involved in 2-DGs anti-endothelial effects related to ER stress induction. Our findings are in agreement with a report by Kim et al, which showed that expression of a constitutively active mutant of GSK3-β induces endothelial apoptosis (49).

The mechanism of GSK3-β activation by ER stress signals is thought to involve dephosphorylation -by protein phosphatase 2A- of the (inhibitory) phospho Ser-9 of the kinase (32). The same mechanism may mediate ER stress induced Akt 473 dephosphorylation, an effect shown in neuronal cells upon induction of ER stress by thapsigargin (32). Meares et al. showed that GSK3-β activation mediates ER stress induced apoptosis by activation of the death inducing transcription factor C/EBP homologous protein (CHOP/GADD153) (33). Taken together, our findings indicate that activation of endothelial GSK3-β by low dose 2-DG may represent a novel and attractive anti-angiogenic strategy.

The in vivo relevance of the above findings was demonstrated in the $LH_{BETA}T_{AG}$ retinoblastoma model, by showing that 2-DG induces the unfolded protein response in vivo, inhibits not only total, but especially newly formed (CD105+) tumor microvessels, and induces endothelial apoptosis in a tumor animal model. This further validates the previous reports by us and others showing that inhibitors of N-linked glycosylation are associated with antiangiogenic and antitumor effects (15, 50). While this study validates the induction of in vivo ER stress and apoptosis after 2-DG treatment, the role of VEGFR2 hypoglycosylation on the in vivo effects is not known. Studies to further characterize the effects of 2-DG on VEGFR2 glycosylation and downstream signaling on in vivo tumor models are underway.

The translational implications of our data are multiple: First, the observation that Akt and Erk inhibition by low dose 2-DG occurs independent of the growth factor used to stimulate ECs suggests that 2-DG, either alone, or in combination, may effectively overcome anti-VEGF resistance in patients treated with these agents. Second, the concentrations of 2-DG used to downregulate endothelial Erk and Akt and induce ER stress are clinically achievable and manifold lower than those needed to induce tumor cell cytotoxicity. A phase I trial of

this drug in combination with chemotherapy (40) showed that plasma concentrations of 2-DG after oral administration are within the range of the concentrations we used (0.6 mM) to inhibit angiogenesis in vitro. This provides a rationale to further develop 2-DG using schedules and modes of administration that reach antiangiogenic concentrations, alone and in combination with other targeted agents. Finally, results from the current study should extend beyond 2-DG. The finding that endothelial cells do not adapt well to ER stress, leading to apoptosis, and the characterization of the pathways involved, can be used to identify agents that may mimic the effects of 2-DG and used as novel antiangiogenics. Several compounds that have been found to be antiangiogenic, such as proteosome inhibitors, tunicamycin, HIV protease inhibitors and statins (at high doses) may mimic some of the effects of 2-DG, either by interfering with glycosylation, or directly inducing ER stress (50-54). Our data, therefore, may provide insight into the potential antiangiogenesis mechanisms of the above agents.

In summary, our studies indicate that the antiangiogenic effects of low dose 2-DG are mediated by its inhibition of N-linked glycosylation, resulting in Erk and Akt downregulation by mechanisms including VEGF receptor hypoglycosylation and induction of endothelial ER stress, leading to GSK3-β activation and apoptosis. Further investigation appears to be warranted to further develop 2-DG as an antitumor-antiangiogenic agent, and to identify drugs that mimic its mechanism of action, to improve the efficacy of, and overcome resistance to currently available anti-VEGF agents.

Supplementary Material

Refer to Web version on PubMed Central for supplementary material.

Acknowledgments

ABBREVIATIONS

2-DG	2-deoxy-D-glucose
2-FDG	2-fluoro-deoxy-D-glucose
EC	endothelial cell
HUVEC	human umbilical vein endothelial cells
HMVEC	human microvascular endothelial cells
eIF2α	eukaryotic initiation factor alpha
ER	endoplasmic reticulum
PERK	PKR-like ER kinase
GRP 78/BiP	78 kDa glucose-regulated protein/Binding immunoglobulin protein
Erk	extracellular signal-regulated kinases

| UPR | unfolded protein response |
| FITC | Fluorescein isothiocyanate |

REFERENCES

1. Folkman J. Angiogenesis: an organizing principle for drug discovery? Nature reviews Drug discovery. 2007; 6:273–86. [PubMed: 17396134]

2. Boere IA, Hamberg P, Sleijfer S. It takes two to tango: combinations of conventional cytotoxics with compounds targeting the vascular endothelial growth factor-vascular endothelial growth factor receptor pathway in patients with solid malignancies. Cancer science. 2010; 101:7–15. [PubMed: 19860846]

3. Hurwitz H, Fehrenbacher L, Novotny W, Cartwright T, Hainsworth J, Heim W, et al. Bevacizumab plus irinotecan, fluorouracil, and leucovorin for metastatic colorectal cancer. N Engl J Med. 2004; 350:2335–42. [PubMed: 15175435]

4. Motzer RJ, Rini BI, Bukowski RM, Curti BD, George DJ, Hudes GR, et al. Sunitinib in patients with metastatic renal cell carcinoma. Jama. 2006; 295:2516–24. [PubMed: 16757724]

5. Sandler A, Gray R, Perry MC, Brahmer J, Schiller JH, Dowlati A, et al. Paclitaxel-carboplatin alone or with bevacizumab for non-small-cell lung cancer. N Engl J Med. 2006; 355:2542–50. [PubMed: 17167137]

6. Rini BI, Atkins MB. Resistance to targeted therapy in renal-cell carcinoma. Lancet Oncol. 2009; 10:992–1000. [PubMed: 19796751]

7. Bhatt RS, Wang X, Zhang L, Collins MP, Signoretti S, Alsop DC, et al. Renal cancer resistance to antiangiogenic therapy is delayed by restoration of angiostatic signaling. Molecular cancer therapeutics. 2010; 9:2793–802. [PubMed: 20699227]

8. Casanovas O, Hicklin DJ, Bergers G, Hanahan D. Drug resistance by evasion of antiangiogenic targeting of VEGF signaling in late-stage pancreatic islet tumors. Cancer Cell. 2005; 8:299–309. [PubMed: 16226705]

9. Pennacchietti S, Michieli P, Galluzzo M, Mazzone M, Giordano S, Comoglio PM. Hypoxia promotes invasive growth by transcriptional activation of the met protooncogene. Cancer Cell. 2003; 3:347–61. [PubMed: 12726861]

10. Merchan JRPH, Qin R, Liu G, Fitch TR, Maples WJ, Picus J, Erlichman C. Final phase II safety and efficacy results of study MC0452: Phase I/II trial of CCI 779 and bevacizumab in advanced renal cell carcinoma. J Clin Oncol. 2011; 29(Suppl) abstract 4548.

11. Motzer RJ, Escudier B, Oudard S, Hutson TE, Porta C, Bracarda S, et al. Efficacy of everolimus in advanced renal cell carcinoma: a double-blind, randomised, placebo-controlled phase III trial. Lancet. 2008; 372:449–56. [PubMed: 18653228]

12. Rini BI, Wilding G, Hudes G, Stadler WM, Kim S, Tarazi J, et al. Phase II study of axitinib in sorafenib-refractory metastatic renal cell carcinoma. J Clin Oncol. 2009; 27:4462–8. [PubMed: 19652060]

13. Datema R, Schwarz RT. Interference with glycosylation of glycoproteins. Inhibition of formation of lipid-linked oligosaccharides in vivo. Biochem J. 1979; 184:113–23. [PubMed: 534512]

14. Kurtoglu M, Maher JC, Lampidis TJ. Differential toxic mechanisms of 2-deoxy-D-glucose versus 2-fluorodeoxy-D-glucose in hypoxic and normoxic tumor cells. Antioxid Redox Signal. 2007; 9:1383–90. [PubMed: 17627467]

15. Merchan JR, Kovacs K, Railsback JW, Kurtoglu M, Jing Y, Pina Y, et al. Antiangiogenic activity of 2-deoxy-D-glucose. PLoS One. 2010; 5:e13699. [PubMed: 21060881]

16. Kurtoglu M, Gao N, Shang J, Maher JC, Lehrman MA, Wangpaichitr M, et al. Under normoxia, 2-deoxy-D-glucose elicits cell death in select tumor types not by inhibition of glycolysis but by interfering with N-linked glycosylation. Mol Cancer Ther. 2007; 6:3049–58. [PubMed: 18025288]

17. Maher JC, Savaraj N, Priebe W, Liu H, Lampidis TJ. Differential sensitivity to 2-deoxy-D-glucose between two pancreatic cell lines correlates with GLUT-1 expression. Pancreas. 2005; 30:e34–9. [PubMed: 15714127]

18. Maher JC, Wangpaichitr M, Savaraj N, Kurtoglu M, Lampidis TJ. Hypoxia-inducible factor-1 confers resistance to the glycolytic inhibitor 2-deoxy-D-glucose. Mol Cancer Ther. 2007; 6:732–41. [PubMed: 17308069]

19. Chan B, Merchan JR, Kale S, Sukhatme VP. Antiangiogenic property of human thrombin. Microvascular research. 2003; 66:1–14. [PubMed: 12826069]

20. Merchan JR, Chan B, Kale S, Schnipper LE, Sukhatme VP. In vitro and in vivo induction of antiangiogenic activity by plasminogen activators and captopril. J Natl Cancer Inst. 2003; 95:388–99. [PubMed: 12618504]

21. Jockovich ME, Bajenaru ML, Pina Y, Suarez F, Feuer W, Fini ME, et al. Retinoblastoma tumor vessel maturation impacts efficacy of vessel targeting in the LH(BETA)T(AG) mouse model. Investigative ophthalmology & visual science. 2007; 48:2476–82. [PubMed: 17525173]

22. Jockovich ME, Murray TG, Escalona-Benz E, Hernandez E, Feuer W. Anecortave acetate as single and adjuvant therapy in the treatment of retinal tumors of LH(BETA)T(AG) mice. Investigative ophthalmology & visual science. 2006; 47:1264–8. [PubMed: 16565356]

23. Jockovich ME, Suarez F, Alegret A, Pina Y, Hayden B, Cebulla C, et al. Mechanism of retinoblastoma tumor cell death after focal chemotherapy, radiation, and vascular targeting therapy in a mouse model. Investigative ophthalmology & visual science. 2007; 48:5371–6. [PubMed: 18055783]

24. Martinet W, Abbeloos V, Van Acker N, De Meyer GR, Herman AG, Kockx MM. Western blot analysis of a limited number of cells: a valuable adjunct to proteome analysis of paraffin wax-embedded, alcohol-fixed tissue after laser capture microdissection. J Pathol. 2004; 202:382–8. [PubMed: 14991905]

25. Mavria G, Vercoulen Y, Yeo M, Paterson H, Karasarides M, Marais R, et al. ERK MAPK signaling opposes Rho-kinase to promote endothelial cell survival and sprouting during angiogenesis. Cancer Cell. 2006; 9:33–44. [PubMed: 16413470]

26. Shiojima I, Walsh K. Role of Akt signaling in vascular homeostasis and angiogenesis. Circ Res. 2002; 90:1243–50. [PubMed: 12089061]

27. Yang B, Cao DJ, Sainz I, Colman RW, Guo YL. Different roles of ERK and p38 MAP kinases during tube formation from endothelial cells cultured in 3-dimensional collagen matrices. J Cell Physiol. 2004; 200:360–9. [PubMed: 15254963]

28. Takahashi T, Shibuya M. The 230 kDa mature form of KDR/Flk-1 (VEGF receptor-2) activates the PLC-gamma pathway and partially induces mitotic signals in NIH3T3 fibroblasts. Oncogene. 1997; 14:2079–89. [PubMed: 9160888]

29. Hicklin DJ, Ellis LM. Role of the vascular endothelial growth factor pathway in tumor growth and angiogenesis. J Clin Oncol. 2005; 23:1011–27. [PubMed: 15585754]

30. Klausner RD, Donaldson JG, Lippincott-Schwartz J. Brefeldin A: insights into the control of membrane traffic and organelle structure. The Journal of cell biology. 1992; 116:1071–80. [PubMed: 1740466]

31. Srinivasan S, Ohsugi M, Liu Z, Fatrai S, Bernal-Mizrachi E, Permutt MA. Endoplasmic reticulum stress-induced apoptosis is partly mediated by reduced insulin signaling through phosphatidylinositol 3-kinase/Akt and increased glycogen synthase kinase-3beta in mouse insulinoma cells. Diabetes. 2005; 54:968–75. [PubMed: 15793234]

32. Song L, De Sarno P, Jope RS. Central role of glycogen synthase kinase-3beta in endoplasmic reticulum stress-induced caspase-3 activation. The Journal of biological chemistry. 2002; 277:44701–8. [PubMed: 12228224]

33. Meares GP, Mines MA, Beurel E, Eom TY, Song L, Zmijewska AA, et al. Glycogen synthase kinase-3 regulates endoplasmic reticulum (ER) stress-induced CHOP expression in neuronal cells. Experimental cell research. 2011; 317:1621–8. [PubMed: 21356208]

34. Wang Q, Zhou Y, Wang X, Evers BM. Glycogen synthase kinase-3 is a negative regulator of extracellular signal-regulated kinase. Oncogene. 2006; 25:43–50. [PubMed: 16278684]

35. Chen CH, Shaikenov T, Peterson TR, Aimbetov R, Bissenbaev AK, Lee SW, et al. ER stress inhibits mTORC2 and Akt signaling through GSK-3beta-mediated phosphorylation of rictor. Sci Signal. 2011; 4:ra10. [PubMed: 21343617]

36. Hughes K, Nikolakaki E, Plyte SE, Totty NF, Woodgett JR. Modulation of the glycogen synthase kinase-3 family by tyrosine phosphorylation. Embo J. 1993; 12:803–8. [PubMed: 8382613]

37. De Bock K, Georgiadou M, Carmeliet P. Role of endothelial cell metabolism in vessel sprouting. Cell Metab. 2013; 18:634–47. [PubMed: 23973331]

38. Fraisl P, Baes M, Carmeliet P. Hungry for blood vessels: linking metabolism and angiogenesis. Dev Cell. 2008; 14:313–4. [PubMed: 18331707]

39. Mohanti BK, Rath GK, Anantha N, Kannan V, Das BS, Chandramouli BA, et al. Improving cancer radiotherapy with 2-deoxy-D-glucose: phase I/II clinical trials on human cerebral gliomas. Int J Radiat Oncol Biol Phys. 1996; 35:103–11. [PubMed: 8641905]

40. Raez LE, Papadopoulos K, Ricart AD, Chiorean EG, Dipaola RS, Stein MN, et al. A phase I dose-escalation trial of 2-deoxy-D-glucose alone or combined with docetaxel in patients with advanced solid tumors. Cancer chemotherapy and pharmacology. 2013; 71:523–30. [PubMed: 23228990]

41. Stein M, Lin H, Jeyamohan C, Dvorzhinski D, Gounder M, Bray K, et al. Targeting tumor metabolism with 2-deoxyglucose in patients with castrate-resistant prostate cancer and advanced malignancies. Prostate. 2010; 70:1388–94. [PubMed: 20687211]

42. Gupta K, Kshirsagar S, Li W, Gui L, Ramakrishnan S, Gupta P, et al. VEGF prevents apoptosis of human microvascular endothelial cells via opposing effects on MAPK/ERK and SAPK/JNK signaling. Experimental cell research. 1999; 247:495–504. [PubMed: 10066377]

43. Nakagami H, Morishita R, Yamamoto K, Taniyama Y, Aoki M, Matsumoto K, et al. Mitogenic and antiapoptotic actions of hepatocyte growth factor through ERK, STAT3, and AKT in endothelial cells. Hypertension. 2001; 37:581–6. [PubMed: 11230338]

44. Zhong D, Xiong L, Liu T, Liu X, Chen J, Sun SY, et al. The glycolytic inhibitor 2-deoxyglucose activates multiple prosurvival pathways through IGF1R. J Biol Chem. 2009; 284:23225–33. [PubMed: 19574224]

45. Nacev BA, Grassi P, Dell A, Haslam SM, Liu JO. The antifungal drug itraconazole inhibits vascular endothelial growth factor receptor 2 (VEGFR2) glycosylation, trafficking, and signaling in endothelial cells. J Biol Chem. 2011; 286:44045–56. [PubMed: 22025615]

46. Chen R, Li J, Feng CH, Chen SK, Liu YP, Duan CY, et al. c-Met function requires N-linked glycosylation modification of pro-Met. Journal of cellular biochemistry. 2013; 114:816–22. [PubMed: 23060267]

47. Contessa JN, Bhojani MS, Freeze HH, Rehemtulla A, Lawrence TS. Inhibition of N-linked glycosylation disrupts receptor tyrosine kinase signaling in tumor cells. Cancer Res. 2008; 68:3803–9. [PubMed: 18483264]

48. Feige JJ, Baird A. Glycosylation of the basic fibroblast growth factor receptor. The contribution of carbohydrate to receptor function. The Journal of biological chemistry. 1988; 263:14023–9. [PubMed: 2844752]

49. Kim HS, Skurk C, Thomas SR, Bialik A, Suhara T, Kureishi Y, et al. Regulation of angiogenesis by glycogen synthase kinase-3beta. J Biol Chem. 2002; 277:41888–96. [PubMed: 12167628]

50. Banerjee A, Lang JY, Hung MC, Sengupta K, Banerjee SK, Baksi K, et al. Unfolded protein response is required in nu/nu mice microvasculature for treating breast tumor with tunicamycin. The Journal of biological chemistry. 2011; 286:29127–38. [PubMed: 21676868]

51. Abcouwer SF, Marjon PL, Loper RK, Vander Jagt DL. Response of VEGF expression to amino acid deprivation and inducers of endoplasmic reticulum stress. Invest Ophthalmol Vis Sci. 2002; 43:2791–8. [PubMed: 12147617]

52. Dulak J, Jozkowicz A. Anti-angiogenic and anti-inflammatory effects of statins: relevance to anti-cancer therapy. Curr Cancer Drug Targets. 2005; 5:579–94. [PubMed: 16375664]

53. Roccaro AM, Hideshima T, Raje N, Kumar S, Ishitsuka K, Yasui H, et al. Bortezomib mediates antiangiogenesis in multiple myeloma via direct and indirect effects on endothelial cells. Cancer research. 2006; 66:184–91. [PubMed: 16397231]

54. Sgadari C, Barillari G, Toschi E, Carlei D, Bacigalupo I, Baccarini S, et al. HIV protease inhibitors are potent anti-angiogenic molecules and promote regression of Kaposi sarcoma. Nat Med. 2002; 8:225–32. [PubMed: 11875492]
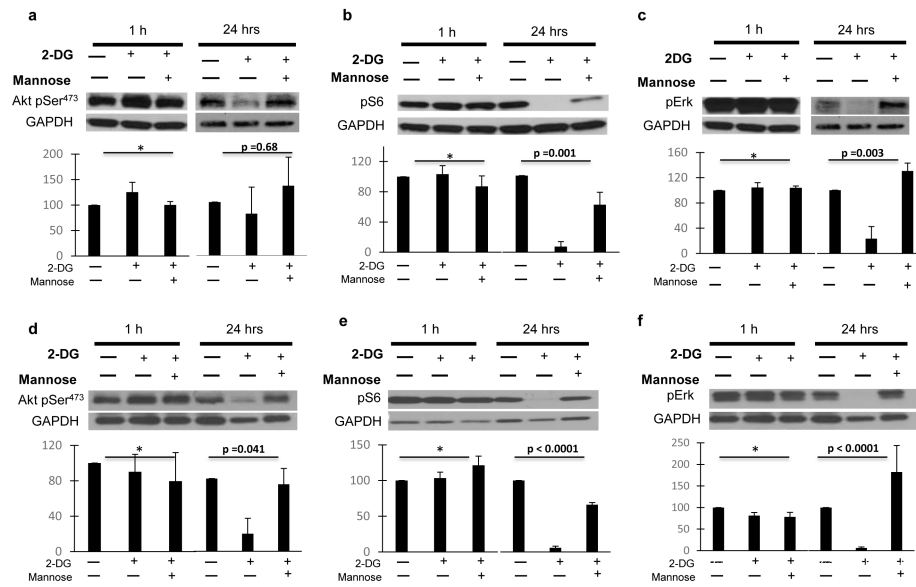
Figure 1. Effects of low dose 2-DG on endothelial PI3K/mTOR and Erk pathways *in vitro*
Starved HUVECs were stimulated with VEGF (**a, b, c**) or bFGF (**d, e, f**), treated with 0.6 mM 2-DG +/− 1mM Mannose, and incubated for 1 or 24 hrs. Lysates were used in standard Western blot procedure (methods). Membranes were then blotted against Akt pSer[473], S6 pSer[240/244], Erk pThr[202]/Tyr[204], and GAPDH as loading control. Band intensity was analyzed by densitometry, normalized to GAPDH, and results displayed as means (+/− SEM) of relative protein density (percent) compared to untreated controls. GAPDH bands from figures 1. a, c and 1. d, f are similar as phosphoproteins were blotted from the same membranes. *p: NS. **: untreated vs 2-DG treated growth factor stimulated HUVECs. Pictures are representative of experiments performed at least in triplicate.
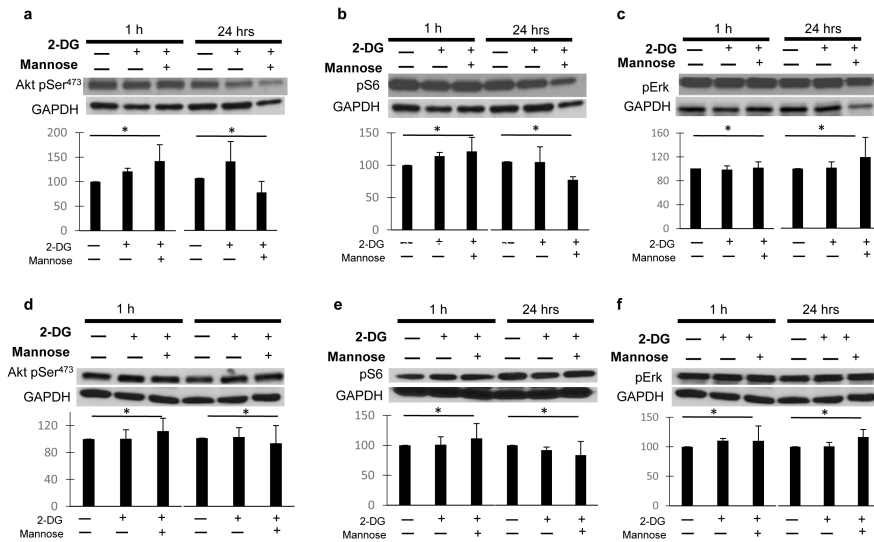
Figure 2. Effects of low dose 2-DG on tumor cell PI3K/mTOR and Erk pathways *in vitro*
MDA-MB-231 (**a, b, c**) and HT-29 (**d, e, f**) cancer cell lines were stimulated with 10% serum, treated with 0.6 mM 2-DG +/− 1mM Mannose, and incubated for 1 or 24 hrs. Lysates were used in standard Western blot procedure (methods). Membranes were then blotted against Akt pSer[473], S6 pSer[240/244], Erk pThr[202]/Tyr[204], and GAPDH as loading control. Band intensity was analyzed by densitometry, normalized to GAPDH, and results displayed as means (+/− SEM) of relative protein density (percent) compared to untreated controls. GAPDH bands from figures 2. a, b and 2. d, f are similar, as the corresponding phosphoproteins were blotted from the same membranes. *p: NS. Pictures are representative of experiments performed at least in triplicate.
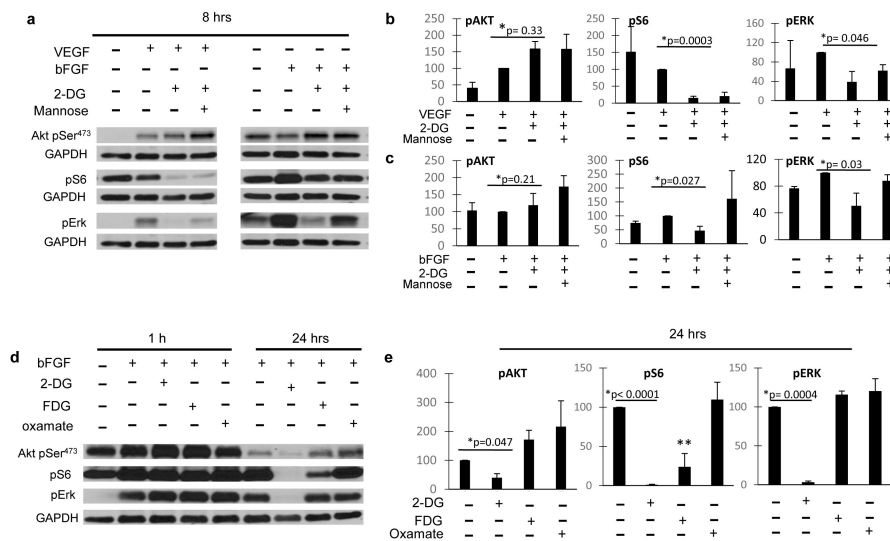
Figure 3. Effects of 2-DG and other glycolytic inhibitors on endothelial Akt/mTOR and Erk
(**a**) Growth factor (VEGF, bFGF) stimulated HUVECs were treated with 0.6 mM 2-DG with or w/o 1mM Mannose and incubated for 8 hrs. Lysates were used for Western blot determination of Akt pSer^{473}, S6 pSer$^{240/244}$, Erk pThr^{202}/Tyr^{204}, and GAPDH as loading control. Band intensity was analyzed by densitometry, normalized to GAPDH, and results displayed as means (+/− SEM) of relative protein density (percent) compared to untreated controls. GAPDH bands corresponding to Akt pSer473 pERK are the same, as phosphoproteins were blotted from the same membrane. Densitometry data are presented from HUVECS exposed to VEGF (**b**) or bFGF (**c**). *: untreated vs 2-DG treated growth factor stimulated HUVECs. (**d**) bFGF stimulated HUVECs were treated with 0.6 mM 2-DG, FDG or oxamate and incubated for 1 or 24 hrs. and levels of Akt pSer^{473}, S6 pSer$^{240/244}$, Erk pThr^{202}/Tyr^{204} were assessed by Western blot. GAPDH loading control is the same for 3 phosphoproteins, as they were blotted from the same membrane. Densitometry data are presented from HUVECs at 24 hours after treatment with 2-DG (**e**). *: untreated vs 2-DG treated growth factor stimulated HUVEC ** p=0.046, FDG vs. control.
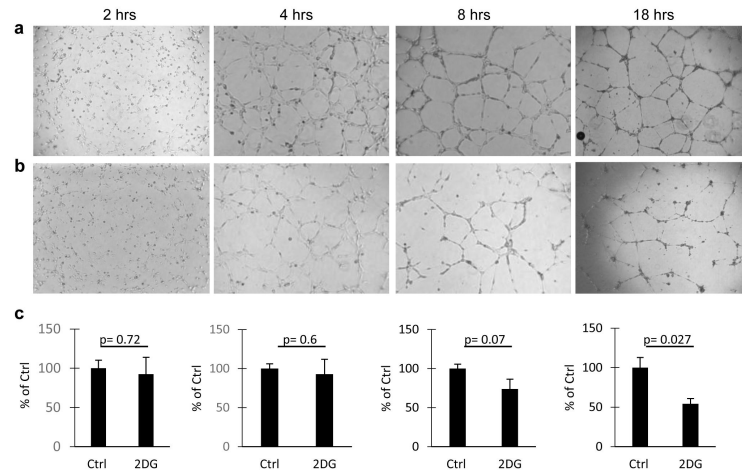
Figure 4. Effects of 2-DG on HUVEC tube formation

HUVECs were plated in matrigel coated wells and treated with PBS (**a**) or 0.6 mM 2-DG (**b**). Tube formation was assessed and photographed at 2, 4, 8, and 18 hours. Scale bar 500μm. (**c**). Quantitative analysis of total tube length was performed as in methods. Histograms represent the average (+/− SEM) tube length (percent of control) of duplicate experiments, repeated at least twice.
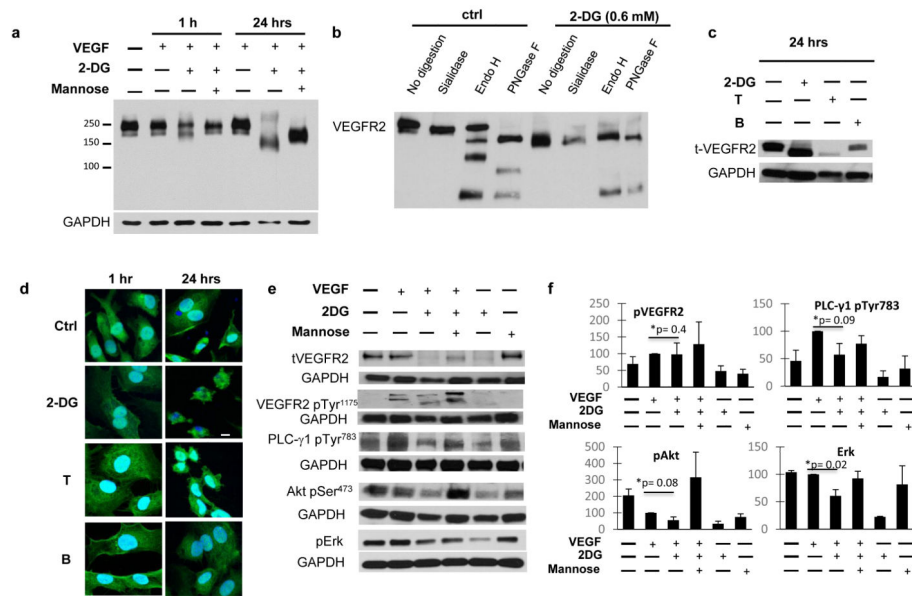
Figure 5. Effects of 2-DG on endothelial VEGFR2

(**a**) HUVECs were stimulated with VEGF and treated with 0.6 mM 2-DG with or w/o 1mM Mannose for 1 or 24 hours. Total VEGFR2 was demonstrated by Western blot analysis, using a low percentage gel to show the complete migration pattern. (**b**) HUVECs were treated with vehicle or 2-DG for 24 hours, and lysates digested with sialidase, endo H or PNGase F, as described in methods. Western blot for total VEGFR2 was performed from digested samples. (**c**) HUVECs were stimulated as above and treated with 2-DG, Tunicamycin (T, 0.25 μg/mL) or Brefeldin A (BFA, 50 nM). Western blot determination of total-VEGFR2 and GAPDH was performed from cell lysates at 24 hours of treatment. (**d**) Endothelial VEGFR2 expression was assessed by Immunofluorescence staining. VEGF stimulated HUVECs were treated with 2-DG, Tunicamycin or Brefeldin as above. Pictures are representative of triplicate experiments. Scale bar: 10 μm. (**e**) HUVECs in starving medium were treated with 0.6 mM 2-DG (+/− 1mM Mannose) for 24 hours, then stimulated with VEGF for 1 hour. Total and phosphor-VEGFR2 (VEGFR2 Tyr^{1175}), activated PLC-γ1 (PLC-γ1 pTyr^{783}), Akt (Akt pSer^{473}) and Erk (Erk pThr^{202}/Tyr^{204}) were assessed by Western blot analysis of cell lysates. (**f**) Band intensity was analyzed by densitometry, normalized to GAPDH, and results displayed as means (+/− SEM) of relative protein density (percent) compared to untreated controls. *: untreated vs 2-DG treated growth factor stimulated HUVECs.
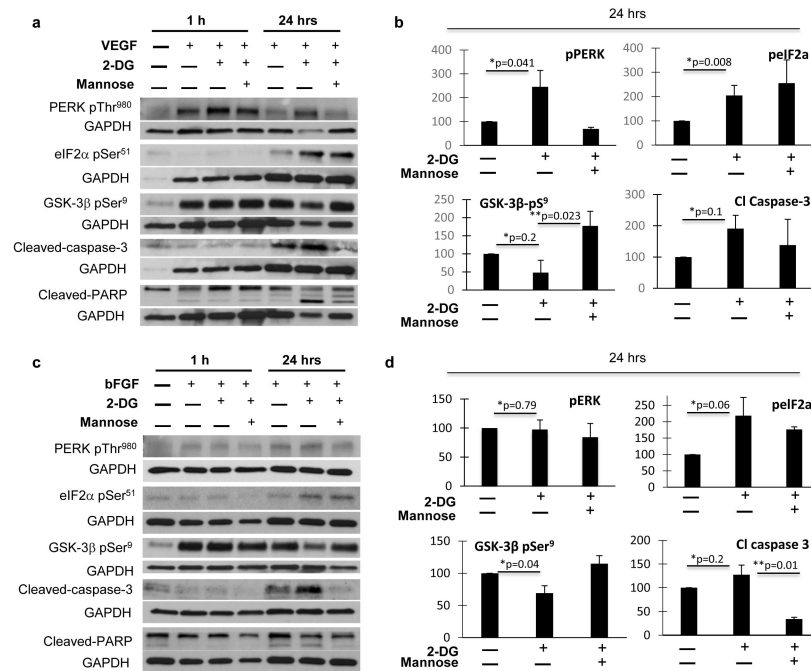
Figure 6. Effects of 2-DG on endothelial endoplasmic reticulum (ER) stress, GSK-3β and apoptosis

a–d: Growth factor stimulated HUVECs (VEGF: **a, b;** bFGF: **c, d**) were treated with 2-DG as described and endothelial ER stress was assessed by activated PERK (PERK pThr^{980}) and eIF-2α (eIF2α pSer^{51}). GSK-3β activation status was evaluated by determination of GSK-3β pSer^9 (inhibitory site) levels. Cleaved-Caspase-3 and cleaved-PARP were assessed to determine apoptosis. Band intensity from 24 hour samples was analyzed by densitometry, normalized to GAPDH, and results displayed as means (+/− SEM) of relative protein density (percent) compared to untreated controls. Fig. 6 and a and c: GAPDH bands corresponding to GSK3β and cleaved PARP, eIF-2α and cleaved caspase 3 (fig. 6. a), and those corresponding to eIF-2α and cleaved PARP (fig. 6. c) are similar, as phosphoproteins were blotted from the same corresponding membranes (for VEGF or bFGF stimulated cells). *: untreated vs 2-DG treated growth factor stimulated HUVECs. ** 2-DG vs 2-DG+Mannose treated, growth factor stimulated HUVECs.
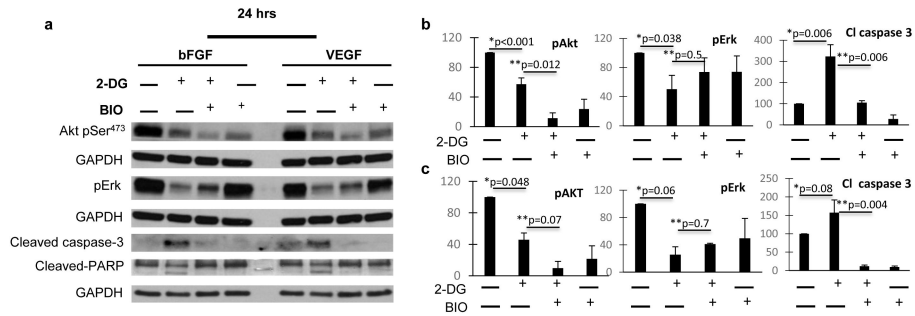
Figure 7. Effects of GSK-3β inhibition on 2-DG induced endothelial AKT/ERK down regulation and apoptosis

Growth factor stimulated HUVECs were treated with 0.6 mM 2-DG with or w/o the GSK-3β inhibitor BIO (5 nM), for 24 hours. Lysates were processed and Akt pSer[473] and Erk pThr[202]/Tyr[204], cleaved-Caspase-3 and cleaved-PARP were demonstrated using standard Western blot procedures (**a**). Densitometry analysis of bFGF (**b**) and VEGF (**c**) exposed HUVECs. GAPDH bands corresponding to pAKT and pERK (for each growth factor) are similar, as phosphoproteins were blotted from the same membrane *: untreated vs 2-DG treated growth factor stimulated HUVECs. ** 2-DG vs 2-DG+BIO treated, growth factor stimulated HUVECs.
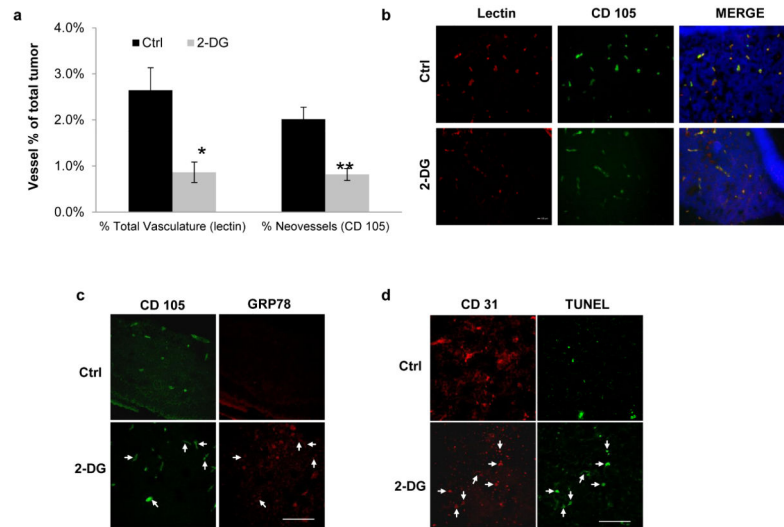
Figure 8. In vivo effects of 2-DG on tumor angiogenesis and induction of unfolded protein response, and apoptosis

LH$_{BETA}$T$_{AG}$ mice were treated with 2-DG or vehicle as described in methods. (**a**) Quantification of tumor microvessel density (total vasculature and neovessels) is presented as percent of total tumor area. Bars represent means +/− SEM of at least 4 independent samples per group. *p= 0.0079, **p= 0.0032 respectively. (**b**) Representative pictures of total and neovessels in control and 2-DG treated samples. (**c**) Tumor samples were stained for GRP78 and CD 105 (endoglin). Arrows represent CD105 and GRP78 positive areas. (**d**) In this experiment, mice were treated for 3 weeks as in methods. Samples were stained for apoptosis (TUNEL) and tumor endothelium (CD31). Representative pictures of experiments performed in quadruplicate. Arrows represent CD31 and TUNEL positive microvessels. Scale bars: 100 μm.

Table 1

2-DG uptake of ^{3}H-2-DG in HT-29 and MDA-MB-231 cancer cells and HUVEC and HMVEC(L)[*].

	Transport rate (nmol/mg protein +/− SD)	
Cells	**5 minutes**	**30 minutes**
HT-29	5.2 +/− 0.69[**]	21.4 +/− 0.67[***]
MDA MB-231	4.1 +/− 0.09	19.2 +/− 0.91
HMVEC(L)	3.2 +/− 0.21	14.9 +/− 0.2
HUVEC	4.0 +/− 0.26	19.7 +/− 1.89

[*] See methods section for description of experiments. HUVEC: Human Umbilical Vein Endothelial Cells; HMVEC(L): Human Lung Microvascular Endothelial Cells; MDA-MB-231: Human mammary Adenocarcinoma; HT-29: Human Colorectal Adenocarcinoma.

[**] p= 0.0086, HT-29 vs HUVEC; p= 0.0005, HT-29 vs. HMVEC.

[***] p= 0.002 HT-29 vs. HMVEC.